XFEL.EU TR-2012-003

CONCEPTUAL DESIGN REPORT

# Framework for X-Ray Photon Diagnostics at the European XFEL

April 2012

*Jan Grünert*

*for the X-Ray Photon Diagnostics Group (WP74) at the European XFEL*

**European X-Ray Free-Electron Laser Facility GmbH**

Albert-Einstein-Ring 19

22761 Hamburg

Germany

European XFEL

# Contents

# Introduction

For the construction of the European XFEL project, the research and development is organized in work packages (WPs). The topic of X-ray photon diagnostics is covered by the X-Ray Photon Diagnostics group (WP74) in the European XFEL GmbH (XFEL.EU)

During the year 2009, WP74 created a general document, "*Concept – Photon Diagnostics for the European XFEL",* which was approved in October 2009 by the European XFEL Management Board. The present document is an update and a more complete successor of this previous document.

The present document takes several new aspects into account:

- New scientific insight and technical consequences from the first lasing of the Linac Coherent Light Source (LCLS) at the SLAC National Accelerator Laboratory in April 2009, which was the first experimental realization of a hard X-ray Free Electron Laser (XFEL) by applying the self-amplified spontaneous emission (SASE) process
- Scientific discussion with future users and X-ray diagnostics experts during several international conferences on this topic, such as the diagnostics workshop at Ryn, Poland, in 2010; the FEL2010 and FEL2011 conferences; and the annual user meetings of the European XFEL
- Major update of the facility layout in March 2011, which adds new operational parameters and extends the beamline energy ranges
- Technical developments in WP74 since 2009

# Document scope

The work in WP74 is organized around the individual diagnostics devices, and therefore their technical concepts are laid out in separate documents with technical details for each device, like conceptual design reviews (CDRs), design reviews (DRs), and other subsequent review documents.

This document on the Global Concept provides a general overview of the work in WP74:

- Creates the framework for the individual device CDRs
- Explains the photon beam properties to be measured
- Gives an overview of the required diagnostics devices and methods, as well as the main application modes of these devices
- Describes the organization of WP74 in terms of budget, staff, and collaborations, including the global optimization strategy to achieve the most and best diagnostics with the available resources
- Explains general issues that are common to all diagnostics devices in WP74

# Related documents

The concepts and technical details for the individual diagnostics devices are covered in separate documents, starting with the CDRs and followed by subsequent review documents as outlined in [Hott 2011].

Currently available or in preparation are the following device CDRs, DRs, and design reports:

- CDR, DR: Undulator Commissioning Spectrometer (*K-Monochromator*)
- CDR: Imaging Stations
- CDR: Photoionization Spectrometer
- CDR: Parasitic Temporal Monitors
- Final DR: Gas Monitor Detector (XGMD)

# Properties of XFEL photon beams

This chapter briefly summarizes the properties of XFEL photon beams, focusing on those of diagnostic relevance.

Before listing beam parameters, we can narrow down the description to a pulsed source in the soft to hard X-ray range.

As in any general description of lasers (see Figure 1), the following properties also apply to XFEL sources:

- Pulse intensity
- Wavelength (center of gravity of the spectrum)
- Spectrum (width, profile)
- Beam position (beam centroid)
- Spot size (and source size) $w(z) = w_0\sqrt{1+(z/z_R)^2}$
- (Far field) divergence $\theta = \frac{\lambda}{\pi w_0}$
- Rayleigh length $z_R = \frac{\pi w_0^2}{\lambda}$
- Degree of transverse / spatial coherence
- Laser modes, $M^2$
- (Local) curvature of the wavefront $R(z) = z\left[1+(z_R/z)^2\right]$
- Pulse arrival time (e.g. relative to an optical laser pulse)
- Pulse duration (and in general longitudinal intensity profile)
- Longitudinal / temporal coherence

In this list, most items are properties of the photon beam and thus distributions; but some items can also be described as properties of the beam-constituting photons, e.g. the individual photon energy.

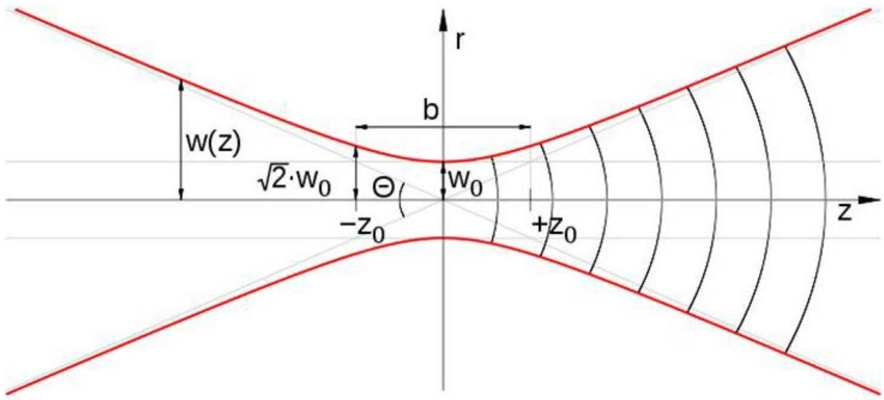


***Figure 1:*** *Laser beam properties at a focus (Source: wikimedia.org)*

Even for a single beam property, the diagnostics will be used under different conditions. There will be different photon wavelengths, intensities, and radiation from one, two, or all undulator segments; single pulse operation or full bunch trains; attenuated or full intensity beam; and commissioning or machine time vs. user operation. Therefore, the device requirements will have several variants.

Certainly, there are good reasons to monitor each of the above-mentioned properties; however, due to limited time, staff, and budget resources, it is necessary to prioritize the properties that can actually be monitored. This prioritization is reflected in the definition of the baseline devices, as shown in Table 5.

These devices will deliver primarily the following diagnostic information:

- Absolute calibrated pulse intensity
- Shot-to-shot (relative) pulse intensity and beam centroid position
- Shot-to-shot central wavelength, spectral width, and degree and orientation of linear polarization
- Offline images (transverse beam position and 2D profile) of spontaneous and FEL radiation
- Offline spontaneous radiation spectrum and transverse profile for individual undulator segments or pairs of undulator segments

For reference, the XFEL beam parameters are given in  and Table 2 [Tschentscher2011]. The coherence properties of the European XFEL are described in detail in [Geloni2010].

***Table 1:*** *XFEL beam parameters of SASE 1 (SASE 2 identical)*

| Parameter | Unit | Value | | | | | | | | | | | | | | | | | |
|---|---|---|---|---|---|---|---|---|---|---|---|---|---|---|---|---|---|---|---|
| Photon energy | keV | 7.75 | | | 12.4 | | | 15.5 | | | 20.7 | | | 24.8 | | | 24.8 | | |
| Radiation wavelength | nm | 0.16 | | | 0.10 | | | 0.08 | | | 0.06 | | | 0.05 | | | 0.05 | | |
| Electron energy | GeV | 14 | | | 14 | | | 14 | | | 14 | | | 14 | | | 17.5 | | |
| Bunch charge | nC | 0.02 | 0.25 | 1 | 0.02 | 0.25 | 1 | 0.02 | 0.25 | 1 | 0.02 | 0.25 | 1 | 0.02 | 0.25 | 1 | 0.02 | 0.25 | 1 |
| Peak power | GW | 46 | 37 | 24 | 35 | 24 | 12 | 29 | 15 | 9 | 21 | 11 | 7 | 15 | 8 | 5 | 25 | 13 | 8 |
| Average power | W | 2 | 23 | 69 | 2 | 15 | 34 | 1 | 9 | 27 | 1 | 7 | 19 | 1 | 5 | 15 | 1 | 8 | 23 |
| Source size (FWHM) | µm | 31 | 39 | 46 | 29 | 37 | 49 | 29 | 35 | 54 | 28 | 39 | 60 | 27 | 42 | 64 | 25 | 36 | 55 |
| S. divergence (FWHM) | µrad | 2.8 | 2.3 | 1.9 | 1.9 | 1.5 | 1.3 | 1.5 | 1.3 | 1.0 | 1.2 | 1.0 | 0.8 | 1.0 | 0.8 | 0.6 | 1.1 | 0.9 | 0.7 |
| Spectral bandwidth | 1E-3 | 2.3 | 1.9 | 1.4 | 1.9 | 1.4 | 1.0 | 1.6 | 1.3 | 0.8 | 1.3 | 0.9 | 0.6 | 1.1 | 0.7 | 0.5 | 1.3 | 0.9 | 0.6 |
| Coherence time | fs | 0.16 | 0.20 | 0.27 | 0.13 | 0.17 | 0.23 | 0.12 | 0.15 | 0.23 | 0.11 | 0.16 | 0.24 | 0.11 | 0.17 | 0.26 | 0.09 | 0.13 | 0.20 |
| Coherence degree | | 0.96 | 0.96 | 0.91 | 0.95 | 0.91 | 0.71 | 0.96 | 0.84 | 0.57 | 0.94 | 0.69 | 0.40 | 0.89 | 0.58 | 0.30 | 0.94 | 0.71 | 0.42 |
| Photons/pulse | 1E11 | 0.6 | 7.0 | 20.7 | 0.3 | 2.8 | 6.4 | 0.2 | 1.4 | 4.0 | 0.1 | 0.7 | 2.1 | 0.06 | 0.5 | 1.4 | 0.11 | 0.8 | 2.2 |
| Pulse energy | µJ | 76 | 864 | 2570 | 58 | 549 | 1260 | 49 | 347 | 991 | 35 | 248 | 708 | 26 | 196 | 558 | 42 | 302 | 863 |
| Peak brilliance | 1E33* | 2.38 | 2.41 | 1.96 | 3.54 | 3.17 | 1.6 | 4.26 | 2.46 | 1.6 | 5.01 | 2.69 | 1.48 | 5.15 | 2.75 | 1.39 | 7.57 | 4.05 | 2.29 |
| Average brilliance | 1E23* | 1.1 | 15.1 | 56.8 | 1.6 | 19.9 | 46.4 | 1.9 | 15.5 | 46.2 | 2.3 | 16.9 | 42.9 | 2.3 | 17.3 | 40.1 | 3.4 | 25.4 | 66.3 |

***Table 2:*** XFEL beam parameters of SASE 3

| Parameter | Unit | Value | | | | | | | | | | | |
|---|---|---|---|---|---|---|---|---|---|---|---|---|---|
| Photon energy | keV | 0.28 | | | 0.496 | | | 1.55 | | | 3.1 | | |
| Radiation wavelength | nm | 4.43 | | | 2.50 | | | 0.80 | | | 0.40 | | |
| Electron energy | GeV | 10.5 | | | 14 | | | 14 | | | 14 | | |
| Bunch charge | nC | 0.02 | 0.25 | 1 | 0.02 | 0.25 | 1 | 0.02 | 0.25 | 1 | 0.02 | 0.25 | 1 |
| Peak power | GW | 105 | 106 | 94 | 118 | 119 | 105 | 90 | 86 | 72 | 73 | 66 | 51 |
| Average power | W | 5 | 67 | 273 | 5 | 75 | 304 | 4 | 54 | 209 | 3 | 41 | 147 |
| Source size (FWHM) | µm | 51 | 65 | 79 | 43 | 56 | 68 | 39 | 50 | 60 | 36 | 46 | 56 |
| S. divergence (FWHM) | µrad | 33.9 | 29.6 | 26.0 | 23.1 | 20.0 | 17.5 | 9.7 | 8.1 | 6.9 | 5.6 | 4.6 | 3.9 |
| Spectral bandwidth | 1E-3 | 6.9 | 6.4 | 5.7 | 5.8 | 5.3 | 4.7 | 4.4 | 3.9 | 3.3 | 3.6 | 3.1 | 2.5 |
| Coherence time | fs | 1.49 | 1.63 | 1.83 | 1.01 | 1.11 | 1.25 | 0.43 | 0.49 | 0.57 | 0.26 | 0.31 | 0.38 |
| Coherence degree | | 0.96 | 0.96 | 0.96 | 0.96 | 0.96 | 0.96 | 0.96 | 0.96 | 0.96 | 0.96 | 0.96 | 0.91 |
| Photons/pulse | 1E11 | 39 | 547 | 2240 | 25 | 347 | 1420 | 6 | 81 | 312 | 2 | 31 | 109 |
| Pulse energy | mJ | 0.2 | 2.5 | 10.1 | 0.2 | 2.8 | 11.3 | 0.2 | 2.0 | 7.8 | 0.1 | 1.5 | 5.4 |
| Peak brilliance | 1E31* | 7 | 7 | 7 | 16 | 17 | 17 | 49 | 54 | 53 | 98 | 104 | 93 |
| Average brilliance | 1E21* | 3 | 46 | 212 | 7 | 109 | 498 | 22 | 338 | 1520 | 44 | 654 | 2680 |

# Diagnostics devices

This chapter describes the diagnostics devices, starting with the various classifications, followed by the main purposes and requirements. Here we aim at providing an overview rather than the full details, which are found in the individual CDRs.

## Device classifications

There are several ways to classify or group the diagnostics devices, which is important since each group shares particular physical principles and technical challenges. The following section also provides the nomenclature for diagnostics devices at European XFEL.

### Complexity

Based on the complexity and method availability, devices fall into one of the following two classes:

- **Baseline devices**

  Will be developed and built first, with the highest priority, and will be available during the initial commissioning of the European XFEL and at the start of operation.

- **Advanced devices**

  Will be developed in parallel to the baseline devices, but will most likely not be available for first-day operation, for one of the following reasons:

  - Underlying physical method is still under scientific debate and, as such, ranks under research rather than technical development.
  - Method is available but currently beyond technical realization.
  - Competent partners have yet to be identified.
  - Devices are simply outside the original scope and budget of the work package.

In general the advanced devices are scientific R&D topics rather than engineering device development.

### Invasiveness

Based on the physical interaction between photon beam and diagnostics, devices are grouped into one of the following classes:

- **Online gas-based devices**

  Mainly applied during user operation, these devices are non-destructive to the photon beam thanks to interaction only with noble gases, such as Neon, Argon, Krypton, or Xenon. By the same virtue, they are themselves indestructible since the ionized gas particles are readily replaced, so there are no issues with single-shot damage or heat load.

- **Online solid-state based devices**

  Mostly for the hard X-ray regime, these devices use a solid target, either thin foils or thicker low-Z bulk material. They have sufficient transmission to permit experimenting or corroborating with a second diagnostics downstream of the first diagnostics device.

- **Invasive devices**

  The main application is during photon beam commissioning and maintenance—these solid-state target based devices completely perturb or absorb the beam. In some select cases, they allow for limited transmission, albeit with a significant effect on the intensity, coherence, and wavefront of the transmitted beam.

### Radiation type: spontaneous vs. FEL radiation

Spontaneous undulator radiation has vastly different properties from the coherent radiation generated in the self-amplified spontaneous emission (SASE) process. The free-electron laser (FEL) radiation has less divergence (on the order of a few microradians), smaller spectral width ($\Delta E/E \sim 10^{-3}$), higher transverse coherence, higher power density, etc. Therefore, the commissioning devices that analyse mostly spontaneous radiation are constructed very differently from the online FEL monitors. They have looser requirements on single-shot damage threshold, pulse-train heat load capability, and spatial resolution; instead, they require higher photon detection sensitivity and a larger transverse detection range.

## Energy range

Depending on the energy range, different techniques are often applicable for the same diagnostics goal. For soft X-rays, the single-shot damage thresholds are much more critical than for hard X-rays, so gas-based methods are preferred. In any case, a UHV environment is mandatory to avoid excessive absorption and scattering in air. For hard X-rays, on the other hand, even online diagnostics is feasible using interaction with solid targets, provided that the average heat load over one pulse train stays manageable.

The energy ranges of the beam transport system and the scientific instruments of the European XFEL were revised in 2011 (see [Tschentscher2011]): the X-ray energy range of the facility was extended down to 260 eV at the lower energies and to 20 keV and beyond at the high energy end. A main energy range and an extended energy range with reduced performance were defined, as shown in Table 3.

***Table 3:*** *Photon energy ranges for the beam transport system and the scientific instruments, including the main and extended energy ranges. (C) and (S) specifies the instrument location on the central (C) or side (S) line of the transport system. Data taken from [Tschentscher2011].*

| Source | Scientific instruments | Main energy range [keV] | Extended energy range [keV] |
|---|---|---|---|
| SASE1 | SPB (C)<br>FXE (S) | 5–20 | 3–5 |
| SASE2 | MID (C)<br>HED (S) | 5–20 | 3–5 |
| | | | 20–36 ([1]) |
| SASE3 | SQS (C)<br>SCS (S) | 0.45–2.0 | 0.26–0.45 |
| | | | 2.0–3.0 |

[1] By using crystal monochromators, energies above 36 keV become accessible.

# Device types

The following section provides an overview of the devices along with brief descriptions, grouped under their classification of invasiveness, as defined in the previous section. The work breakdown structure of WP74 is based on these device groups and devices.

For a key to the icons in this section, see Figure 5 on page 26.

## Online devices (gas-based)

A common feature of gas-based online devices is the excellent online capability during user operation thanks to the weak interaction of X-ray photons and rare gases. These devices are indestructible by design, since the photon beam interacts only with a continuously replenished gas target.

### *X-ray gas monitor detector (XGMD) and beam position monitor (XBPM)*

Rare gas atoms are ionized by X-ray photons transmitted through the detection volume. The generated ions and electrons are detected by two opposing electrodes, electron-multipliers, or both. The output of this device is an absolutely calibrated value of the XFEL pulse intensity (number of photon per pulse) and the transverse (x, y)-position from the XBPM. Two sets of these devices per undulator (placed before and after the attenuators) deliver online shot-to-shot data to users. These monitors are provided by HASYLAB. For details, see [Tiedtke2008, Sorokin2011].

### *Photoemission spectrometer (PES)*

As in the XGMD, the passing X-ray photons ionize a rare gas, and the resulting photoelectrons are detected in time-of-flight (ToF) spectrometers. The ToF-spectrum can be converted to a photon energy scale. Secondary information is the beam polarization, when the photoemission is recorded simultaneously in several different angles perpendicular to the photon beam axis. The device is also called a “photoionization spectrometer” or simply an “online spectrometer”. For details, see [Buck2012].

## Online devices (solid-state based)

The original planning and budget did not account for solid-state-based online devices. However, in the last few years, interesting devices appeared to become feasible that allow us to monitor intensity, beam position, or both in a semi-transmissive way and still provide sufficient potential for radiation hardness. Previously, silicon-based transmissive X-ray diodes were developed [Fuchs2008] and already commercially marketed [Micron2009]. Thinned-down (5–10 µm) transmissive silicon position-sensitive detectors have ~ 95 % transmission at 12.4 keV. At synchrotrons, a submicron position resolution was demonstrated at measurement rates of up to 1 kHz (S/N = $6 \cdot 10^4$ at 10 Hz). However, as reported by users[2], their lifetime is much too short (on the order of hours to days) even when subjected only to the modest radiation levels of monochromatized synchrotron beamlines.

Much more promising for application in intense XFEL beams are the diamond-based detectors, where the X-rays are directly detected by charge generation and pA-meters. It is important to note that, for their application at XFELs, special contact materials and geometries can help to circumvent single-shot damage[3]. The strategy here is to develop some prototypes with a small budget, to qualify their application at low rep-rate XFELs, and then to provide the design to the experiment groups of the scientific instruments, which are particularly interested in these devices as they could provide relative shot-to-shot intensity and beam position monitoring in a very compact and robust fashion as compared to the bulky and involved gas-based systems.

[2] Various EMBL users of photon sources at HASYLAB (private communication)

[3] Before damage by melting occurs, diamond will graphitize. This effect and "heat bumping" of diamond structures are subject to further studies.

### *Diamond detectors*

A solid-state equivalent of a gas ionization chamber, the diamond detectors can—depending on electrode configuration—provide beam position (“Diamond PSD”) and intensity information (“Diamond $I_0$-monitor”). At a suitable combination of photon energy and slab thickness, the transmission can be sufficient to perform further diagnostics downstream of the detector or to use the transmitted beam for experiments, as long as those experiments can tolerate the modification of beam coherence and wavefront. The X-rays create electron-hole pairs in the diamond that are directly detected as a current, as demonstrated at synchrotron radiation (SR) sources [Schulze-Briese2001, Bergonzo2006, Pomorski2009]. With sensitive high-bandwidth front-end electronics [Moritz2001] and fast DAQ, even pulse-resolved measurements at 4.5 MHz in a pulse train are feasible. The importance of space charge or charge cloud effects caused by the intense XFEL pulses has yet to be experimentally tested.

### *Backscattering monitor (BSM)*

In the backscattering monitor (BSM), X-rays are transmitted through a thin foil, so only little intensity is lost. The X-rays scattered backwards from the foil are detected by photodiodes upstream of the foil. Four diodes placed symmetrically around the beam allow for determining photon beam position and relative pulse intensity on a shot-to-shot basis. The BSM is therefore a position-sensitive detector (PSD).

Developed for XFELs originally within the LUSI program at SLAC, the backscattering foil monitor has been applied not only as a standard device for intensity and position monitoring [Feng2009] in the hard X-ray hutches of LCLS at SLAC, but was further developed in a collaboration between SLAC and Super Photon ring-8 GeV (SPring-8) using diamond foils [Tono2011]. A theoretical investigation at European XFEL, including simulations of the back-scattered fields and the heat load effects during pulse trains, analysed the potential of such devices for the European XFEL, and the positive results supported further development towards our own prototypes [Volkov2011]. A CDR for the BSM is planned for autumn 2012.

Common to all these devices is the limited application range in terms of pulse energy density during XFEL pulse trains. These devices can be employed freely only in the monochromatic beam, attenuated beam, or both, but can provide shot-to-shot data. Depending on photon energy, a careful selection of the foil material can push the heat load damage threshold such that even long pulse trains can be accepted, as shown in Figure 4.

***Table 4:*** *Heat load damage thresholds for the BSM for different foil materials—calculation results [Volkov2011]*

| | | Average Heat Load | Pulse Train Mode | | | | | | | | |
|---|---|---|---|---|---|---|---|---|---|---|---|
| | | X-ray energy 7.75 keV | X-ray energy 7.75 keV | | | X-ray energy 12.4 keV | | | X-ray energy 20.7 keV | | |
| | | Pulse energy 2.57 mJ | Pulse energy 2.57 mJ | | | Pulse energy 1.26mJ | | | 0.708mJ | | |
| | T melt,C | ΔTcond,C | ΔT train | ΔTcond | Nmax | ΔT train | ΔTcond | Nmax | ΔT tr | ΔTcond | Nmax |
| Diamond | 3550 | 7,8 | 5243 | 1319 | whole train | 616 | 155 | whole train | | | |
| Silicon Nitride | 1414 | 1109,3 | 228905 | 187800 | 17 | 27951 | 22931 | 137 | 3496 | 2868 | 1092 |
| Be | 1415 | 11,4 | 546 | 1937 | whole train | 83 | 295 | whole train | | | |
| Boron Carbide | 2445 | 217,9 | 2486 | 36889 | 2655 | 314 | 4661 | whole train | | | |

## Invasive / commissioning devices

Invasive / commissioning devices include MCP-based detectors, an undulator-commissioning spectrometer, 2D imagers, pop-in monitors, a single-shot spectrometer, a wavefront sensor, and a pulse duration monitor.

E

### *MCP-based detector*

An MCP-based detector is based on multi-channel plates (MCPs) and consists of two main components:

- Direct illumination of spatially integrating MCPs delivers an integral value for the shot-to-shot pulse intensity (number of photons per pulse).
- MCP imagers, where the amplified electron signal is converted by a phosphor screen into an optical signal, deliver a spatial image of the photon beam at a 10 Hz CCD repetition rate.

While a bolometer or thermopile is useful only for small intensities, the pulse intensity measurement with MCPs has a very large dynamic range. It can be used during the SASE search to find slight increases above the spontaneous signal with ~ 1% relative accuracy; and, once the FEL is established, it can characterize the gain curve up to full saturation by gain-adjusting through the

HV supply and by using detuned beamline offset mirrors as X-ray attenuators. More on the development of MCP-based detectors is found in [Bychkov2004, Bittner2007], more on the design for the European XFEL in [Syresin2011].

### *Undulator-commissioning spectrometer (K-monochromator)*

The K-*monochromator* is a two- or four-bounce crystal monochromator with two channel-cut Silicon crystals, which allows the precise setting of undulator segment gaps and phases. To enable lasing, the differences of undulator parameter *K* between segments have to be minimized and the phases between segments need to be adjusted. Also, such a spectrometer is the only way to check in situ the magnetic field of individual undulator segments after installation in the tunnel and to set up calibration tables. This could be repeated periodically during operation to identify segments with deteriorated performance.

### *2D imagers*

In each SASE undulator beamline, there is one high-performance imager dedicated to measuring the 2D transverse beam profile of the spontaneous and also the FEL radiation. It can visualize the direct beam at typical CCD camera acquisition rates (on the order of 10 Hz); in combination with the *K*-monochromator, it constitutes the spatially resolving undulator commissioning spectrometer.

Great efforts are made to develop large, ultrafast, pixelated 2D detectors for direct X-ray imaging. These sophisticated detectors will record several hundred images during one pulse train and will be available for user experiments rather than for basic X-ray photon beam diagnostics. It will not be possible to acquire full frame images at the intra-pulse-train repetition rate of 4.5 MHz with commercially available cameras, but the imagers will rather deliver data at 10 Hz during commissioning.[4]

---

[4] Fast, state-of-the-art, 2D detectors allow for the acquisition of *two* images during *one* individually selected 600 µs long pulse train: (a) Interline transfer CCD cameras produce *two* fast successive images in gated dual-image mode without an external shutter at exposure times as low as 100 ns. The charge transfer from imaging pixels into shielded storage pixels typically takes 1 ms and the readout about 7 ms. (b) Intensified digital (12-bit) CCD cameras record *two* discrete images with an interframing time of 500 ns at exposure time settings from 3 ns to 1000 s. Fast phosphor decay times to 10% of the initial intensity are

Cameras with gated detection are expensive, but one imager per beamline might be equipped with such a detector to observe the lasing of an arbitrary single pulse in a train and to pick out a particular pulse in a pulse train for wavefront sensing. The operation mode with pulse trains will require cooling of this device.

### *Pop-in monitors*

Simple retractable imaging monitors, known as pop-in mirrors, are needed to precisely align devices along the very long photon beamlines. They consist of a scintillator, optics, and an optical camera. They are placed adjacent to any X-ray optics in the beamline. Specified to work with an FEL beam in single-bunch mode (10 Hz), their design is driven by simplicity and cost-effectiveness, as they are numerous and used only offline (not during user operation).

### *Single-shot spectrometer (SSS)*

For single-shot analysis of the spectrum at the European XFEL, WP74 is actively investigating the following proposed concepts:

- **Dispersive crystal setup**

  In this design [Yabashi2006], the beam is focused by a curved mirror, and then a flat crystal creates a spatially resolved spectrum on a 2D detector.

- **Fresnel zone plates**

  Either transmissive or reflective zone plates could combine the functionality of focusing and dispersing in the same X-ray optics element, thus reducing the number of elements. In experimental studies [David2011], the damage thresholds and the performance of these elements is tested.

Both concepts are studied and compared by ray-tracing simulations [Rehanek2011] to find the optimal configuration and to understand their application range. Full single-shot spectrum information is mandatory for seeded FEL operation.

---

0.2–0.4 μs (down to 1% in 2 μs). Severe limitations are given by the grain size of the screens, wavelength characteristics, and detection efficiency.

### *Wavefront sensor*

There are currently two main concepts for wavefront analysis relevant for diagnostics; a third, novel approach is under investigation.

The following two concepts are well established:

- **Hartmann plate wavefront sensor** [Schäfer2002]:

  For the XUV range, this is the common solution and it is successfully applied at FLASH for routine diagnostics. Proof-of-principle tests confirmed, that Hartmann plate based sensors could also be used with slight adaptations for soft X-rays, but our own tests [5] with hard X-rays at PETRAIII showed strong limitations, mainly concerning difficulties in calibration. However, there exists one commercial product [6] for hard X-rays.

- **Interferometric grating wavefront sensing**

  Using a Moiré technique (see Figure 2), complete wavefront information can be recorded with an angular sensitivity down to 10 nrad, corresponding to hard X-ray wavefront distortions smaller than λ /10.

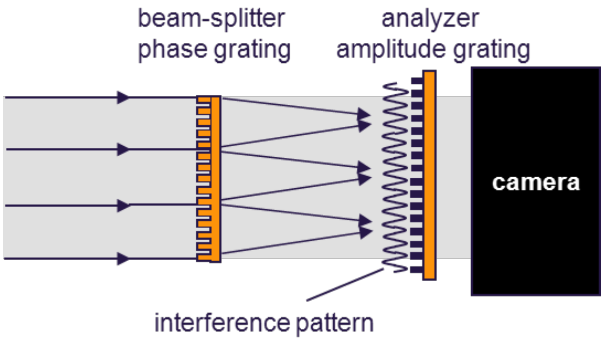


***Figure 2:*** *Schematic setup of a grating interferometer (source: C. David, PSI)*

The wavefront of the FEL radiation itself is determined—even in single-shot mode, disturbing effects of additional optics are evaluated—and the transverse and longitudinal photon source position in the undulator can

[5] Commissioning Beamtime at PETRA III, beamline P10, at DESY in July 2010. Principal collaborators: Michael Sprung (DESY), Bernhard Flöter and Klaus Mann(Laserlabor Göttingen LLG), WP74.

[6] HASO-X from Imagine-Optic (35 µm thick Gold Hartmann plate, 8 µm size square holes turned by 25°, 20 µm spatial resolution, 0.9 × 0.7 mm² useful area, 45 × 35 measurement points)

be assessed. The focal spot size and the wavefront in the beam waist are characterized by measuring the divergent beam behind refractive focusing devices, e.g. compound refractive lenses (CRLs).[7]

In addition to these two well-established techniques, a third approach has being investigated since spring 2011 in a collaboration between CXI at LCLS, the Scientific Instrument SPB group at the European XFEL, and WP74:

- **Phase determination via longitudinal intensity gradient / non-interferometric phase imaging** [Paganin1998]

  Using this approach, three successive screens (Ce:YAG scintillators and thin Al-coated $Si_3N_4$ membranes as optical mirrors transparent to X-rays) are placed behind the focus of an experiment, as shown in Figure 3. Three cameras outside the vacuum chamber record the beam spots, and phase propagation calculations with the images finally yield the longitudinal intensity gradient.

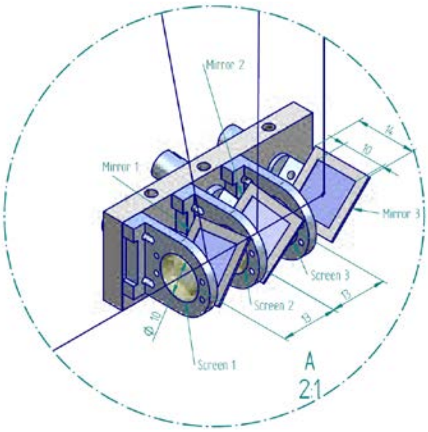


***Figure 3:*** *Workshop drawing of the initial test assembly for the "three-screen method"*

All three methods are restricted in repetition rate by the camera acquisition, but the expectation is to use gated detection to study pulse train effects by stepping the gate through the pulse trains, and eventually to allow for multiple acquisitions within one pulse train.

---

[7] Beamtime in October 2010 at XPP at LCLS at SLAC. Principal collaborators: C. David (PSI in Switzerland), D. Fritz (SLAC in USA), H. Sinn (European XFEL, WP73), and J. Grünert (European XFEL, WP74).

## Coherence monitor

Several methods have been proposed for the coherence monitor, but no simple robust diagnostics method has been established to date. A typical FEL method in the XUV is to record the diffraction pattern of a double slit and to measure the visibility of the interference fringes [Ischebek2004]. Another method demonstrated at synchrotrons uses dynamical near-field speckles formed by scattering from colloidal particles [Alaimo2009].

## Temporal diagnostics

Monitoring temporal properties of the XFEL photon beam is a wide field of active scientific research. The general strategy of WP74 aims at acquiring know-how in this topic through involvement in collaborations and in providing assistance to other European XFEL groups involved in time-resolved measurements, rather than prematurely attempting device development and engineering. The physical realization of this diagnostics will be mainly organized by the instrument groups, since most temporal diagnostics measurements need to be integrated into the experiment itself.

In brief, the two properties in closest reach for a diagnostic measurement of temporal photon pulse properties, at least on a 10 Hz level, are the pump-probe arrival time and the pulse duration.

### *Arrival time monitor*

Monitoring of the delay between the arrival of X-ray photons and an optical laser pulse is required for pump-probe experiments. One method is to record the X-ray-induced change of the optical index of refraction in a thin target, where the arrival time can be spatially or spectrally encoded in a reflected or transmitted optical laser beam.[8] In spectral encoding [Bionta2011], the spectrum of an optical laser is chirped and the transmitted spectrum that contains a signature of the relative arrival time is recorded. Both variations allow for a parasitic arrival time monitoring that is, however, limited to typical CCD repetition rates.

[8] Beamtime in October 2011 at SXR at LCLS at SLAC. Principal investigator: William Schlotter (SLAC in USA).

### *Pulse duration monitor*

The photon pulse duration is adjustable through the electron bunch charge. Several methods have been proposed, of which streaking the electron bunch after passage of the undulator seems to have the highest potential in terms of time resolution [Ding2012]. A transverse deflecting cavity streaks the electron bunch after it is used for lasing in the undulator. The temporal intensity profile of the photon pulse is derived by comparison with electrons that have passed the undulator but have been prohibited from lasing. This kind of monitor would be part of the electron machine and is not within the scope of WP74.

Many more methods under active investigation concerning diagnostics of temporal properties of the European XFEL are described in [Li2012].

# Summary tables

The following tables summarize the baseline devices as outlined in the European XFEL TDR [Altarelli2006], the advanced diagnostics devices, and additional developments that are useful for and could be adopted by the scientific instruments.

***Table 5:*** *Summary of baseline diagnostics at the European XFEL*

| Device | Monitored property | Shot to shot | FEL pulses per train | Online device | Absolute value |
|---|---|---|---|---|---|
| XGMD | Intensity | X | Full train | X | X |
| XBPM | Position | X | Full train | X | – |
| Photoionization spectrometer | Spectrum, polarization | X | Full train | X | X |
| MCP-based detector | Intensity | X | < 30 | – | – |
| | 2D image | – | 1 | – | – |
| *K*-monochromator | Spectrum | – | Few | – | – |
| 2D imager | 2D image | – | 1 | – | – |
| Pop-in monitor | 2D image | – | 1 | – | – |

***Table 6:*** *Advanced devices*

| Device | Monitored property | Single shot | Pulses per train | Online device | Absolute value |
|---|---|---|---|---|---|
| Pulse-resolved wavefront sensor | Wavefront | X | 1 | X | – |
| Single-shot spectrometer | Spectrum | X | 1 | (X) | – |
| Transverse coherence monitor | Transverse coherence | X | ? | X | – |
| Photon BAM | Beam arrival time | X | Full train | X | X |
| Pulse duration monitor | Pulse duration | X | < 30 | – | – |

***Table 7:*** *Additional device/method developments*

| Device | Monitored property | Shot to shot | Pulses per train | Transmissive |
|---|---|---|---|---|
| Diamond detector "$I_0$-monitor" | Intensity | X | Full train | X |
| PSD diamond detector | Intensity | X | Depends on photon energy | X |
| | Beam position | X | | |
| Backscattering foil monitor (BSM) | Intensity | X | Depends on photon energy and foil material | X |
| | Beam position | X | | |

***Table 8:*** *Work Breakdown Structure (WBS) for WP74, based on the device groups and devices as defined in this chapter*

| **Device group** | **PSP element** | **Item** | **Device name** |
|---|---|---|---|
| Online devices (gas based) | P.02.03.74.11 | 11-1 | XGMD |
| | | 11-2 | XBPM |
| | | 11-3 | PES/OPS |
| | | 11-4 | Infrastructure for gas based online devices<br>Integration |
| Online devices (solid state) | P.02.03.74.21 | 21-1 | Diamond $I_0$ monitor |
| | | 21-2 | Diamond PSD |
| | | 21-3 | Backscattering PSD |
| | | 21-4 | Infrastructure for solid state online devices<br>DAQ and Control |
| Commissioning / destructive devices | P.02.03.74.31 | 31-1 | MCP-based detector |
| | | 31-2 | *K*-monochromator |
| | | 31-3 | 2D imager |
| | | 31-4 | Pop-in monitors around optics |
| | | 31-5 | Single-shot spectrometer |
| | | 31-6 | Hartmann wavefront sensor |
| | | 31-7 | Grating interferometer |
| Timing diagnostics | P.02.03.74.41 | 41-1 | Optical reflectivity change (pump-probe delay) |
| | | 41-2 | Sideband generation |
| | | 41-3 | Other timing diagnostics |
| Coherence | P.02.03.74.51 | 51-1 | Coherence monitor |
| Non-device items | P.02.03.74.61 | 61-1 | Project management |
| | | 61-2 | Infrastructure |
| | | 61-3 | Documentation |
| | | 61-4 | Simulation of spontaneous radiation |
| Recurrent cost | P.02.03.74.01 | 01 | Trainings, travel, fees, etc. |

# Location in the facility

This section presents the number of devices per type and their locations.

## Online devices (gas-based)

The contracted number of *XGMDs and XBPMs* currently provides two intensity and two (x, y)-position measurements per undulator, placed before and after the attenuators and slits to monitor the "pure" delivered beam from the undulator with the first set and the tailored attenuated beam with the second.

To measure the intensity arriving at the user experiment after transmission through the beam transport system, another intensity measurement in the scientific instrument is required. To reduce complexity and cost, this could be a relative measurement on a shot-to-shot basis, with an initial characterization by a calibrated device.

The calculation of the absolute intensity value from the XGMD measurement data implicitly assumes the linear regime, so the XGMD may not be positioned near a focus or too close to the undulator exit. The minimum beam diameter is defined by the saturation effect upon photoionization, which depends on the number of photons per pulse and photoionization cross section.

The minimum beam diameter at which this affects the measurements by 1% is estimated to be:

- 16 µm at a photon energy of 12.4 keV
- 0.18 mm at a photon energy of 3.1 keV
- 3.2 mm at a photon energy of 0.25 to 0.7 keV

With beam divergence and source size values for the respective beamlines taken from the TDR, the minimum distances from the undulator are 37 m and 260 m for SASE2 and SASE3 beamlines, respectively. For SASE1, the minimum distance is not relevant because the saturation effect arises at a beam diameter of less than 16 µm, which is smaller than the source size. Another limit is imposed by the minimum distance required to sufficiently suppress spontaneous radiation. These minimum beam diameters and the related minimum distances were calculated for Xenon as a target gas. For other gases (e.g. Krypton or Argon), these values will be different.

The characteristics of the spontaneous radiation at the placement location are also important: the XGMD is sensitive to radiation in a broad spectral range depending on photoionization cross sections. Generally, it becomes more and more sensitive as the photon energy decreases because of increasing photoionization cross sections. The spontaneous radiation has a broad spectral distribution and a divergence of about 0.1 mrad. If we compare the divergence of spontaneous radiation beam to the SASE FEL beam, which is of about few microradians, then it is clear that the unwanted spontaneous radiation is suppressed by placing the XGMDs as far from the undulator as possible and preferably after a set of small apertures. Additionally, the spontaneous radiation is suppressed by using a gas attenuator that will cut low photon energies. However, this might also affect the quality of the SASE beam.

For all considerations concerning XGMD placement see [Grünert2009-2].

One *PES* is allocated per undulator, positioned downstream of the offset mirrors to avoid the spontaneous radiation and Bremsstrahlung background that would also negatively affect its sensitive electronics. Ideally, since there are monochromators planned downstream of the distribution mirrors, one would build such an online spectrometer upstream of each of the six scientific instruments, which is unfortunately not covered by the diagnostics budget. For more details about the PES placement, see [Buck2012].

### Online devices (solid-state based)

These devices could be added on retractable paddles where needed, but their main application is in the beamline downstream of monochromators and in the scientific instruments, where they could save precious space compared to gas-based devices, albeit at the expense of limited applicability during pulse trains.

### Invasive / Commissioning devices

Commissioning devices that are used with spontaneous radiation essentially have to be placed upstream of the radiation protection offset mirrors. One exception to this rule is the *MCP-based detector,* which is located directly adjacent and downstream of the second offset mirror, and which is designed such that it can be operated with both mirrors in the beam, with one mirror in the beam, or with no mirror in the beam. Therefore, it can initially also receive the spontaneous radiation during the first SASE searches. After FEL is found, introducing the mirrors is then used to reject high-energy spontaneous and Bremsstrahlung radiation and to attenuate the FEL. Exceeding the regular mirror angles for user operation will allow further attenuation.

For more about the placement and operation of the MCP-based detector, see the design report by the contributing institute JINR in Dubna [Syresin2011].

The *imager* is placed adjacent and downstream of the *K*-monochromator constituting the *undulator commissioning spectrometer*. Together, they are placed just upstream of the offset mirrors and downstream of the attenuators and slits to have access to their beam shaping functionality. There is one undulator commissioning spectrometer per undulator beamline.

The set of invasive devices is completed by the retractable *pop-in monitors* that provide beam images near each X-ray optics element. A special version of these monitors is the *transmissive imager*, which is provided once per beamline. It is placed as close to the undulator as possible (immediately downstream of the electron beam separation), and will be operated simultaneously with the 2D imager at the *K*-monochromator to provide beam pointing information.

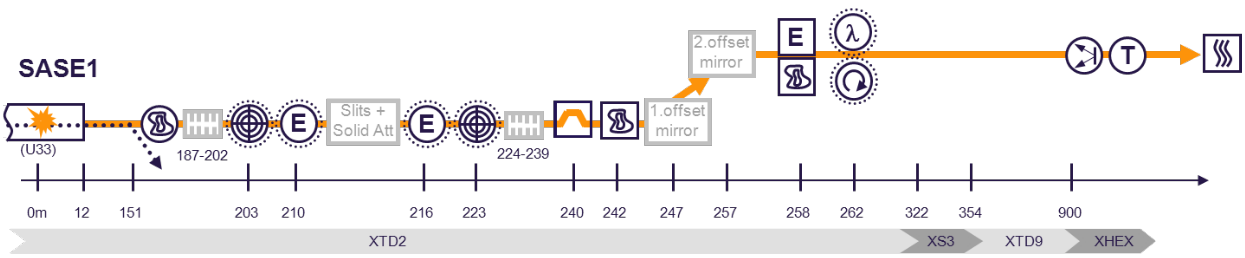


***Figure 4:*** *Location of diagnostics devices as shown in Figure 6.*

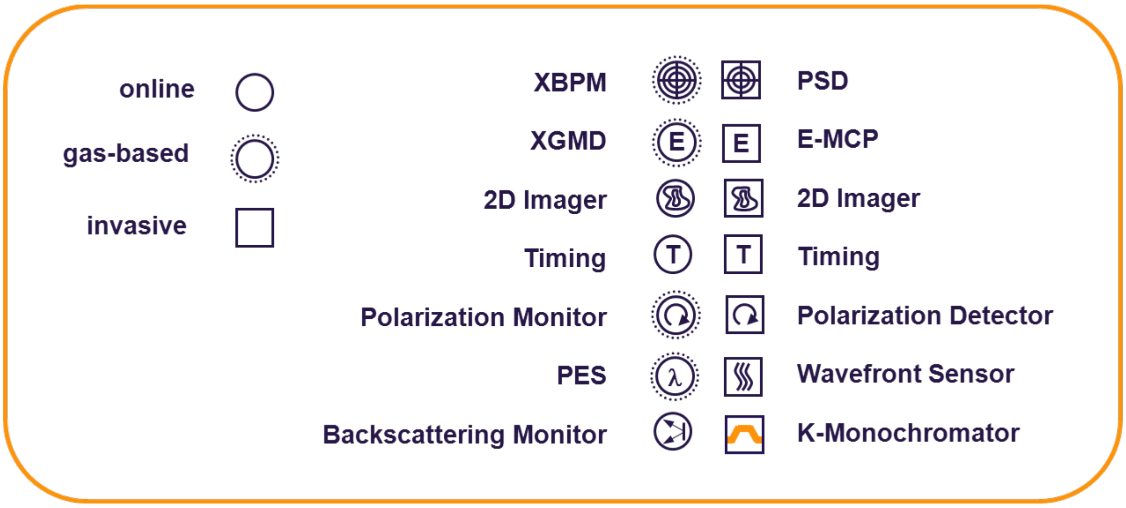


*__Figure 5:__ Legend with symbol descriptions used in "Device types" on page 11 as well as in Figure 4 and Figure 6.*

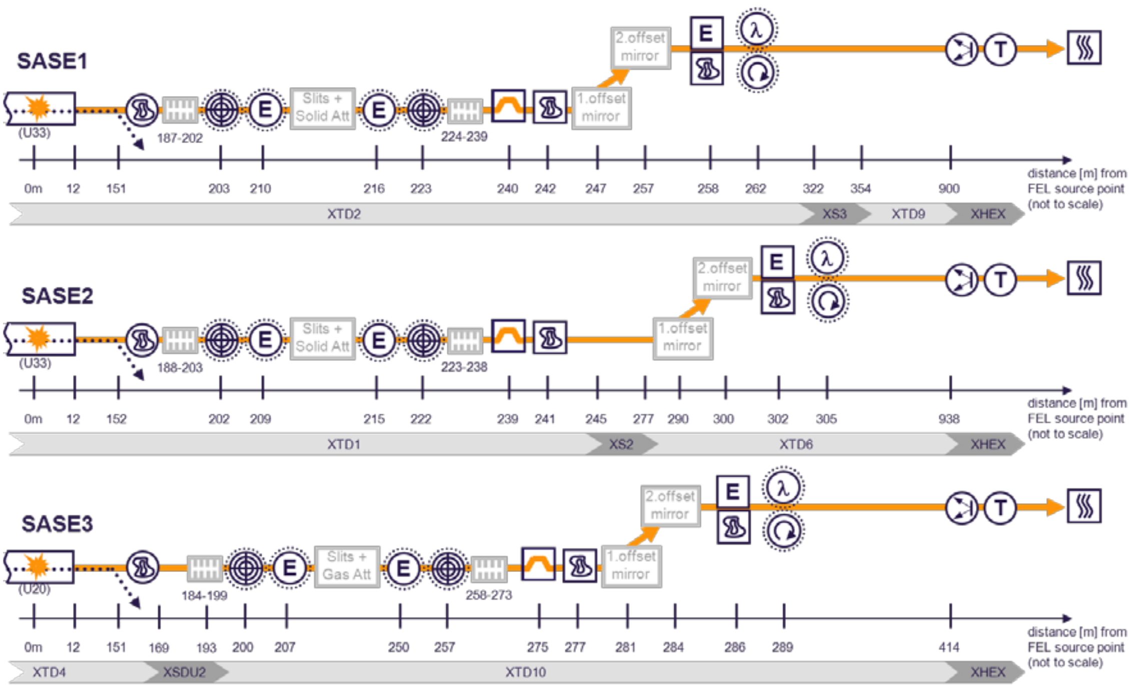


*__Figure 6:__ Location of all diagnostics devices in the facility. For clarity, pop-in imagers are not shown. For more explanations, see the caption of Figure 4. For the symbol legend, see the caption of Figure 5.*

# Requirements

By principle, diagnostics requirements are limited by resources rather than by demand. With unlimited resources, one could provide devices for each diagnostic parameter or physical quantity, optimized for the particular energy, position in the beamline, etc. Therefore, the art of diagnostics is in providing the optimum amount of information about the photon beam with a given set of resources and within the limitations of current technical feasibility.

The set of basic requirements for the European XFEL facility diagnostics given here is largely based on [Grünert2009] and is reiterated per device in the respective conceptual design reports.

## Commissioning requirements

This section describes the commissioning requirements for pulse intensity; photon beam position; transverse beam profile, shape, and position; total energy in the radiation pulse and photon beam image; spectral content; and spectrum.

### Pulse intensity

The flux (number of photons/s) has to be measured from low intensity spontaneous radiation up to FEL saturation, directly in front of and behind the attenuators to derive the attenuation factor, and close to experiments to determine beamline optics losses and the intensity delivered to the user target. The temporal resolution is required to exceed 180 ns to resolve with certainty individual pulses in pulse trains.

***Table 9:*** *Requirements for intensity measurements*

| Parameters | Requirements | Type of measurement |
|---|---|---|
| Measurement uncertainty | < 10% | Absolute measurement |
| | < 1% | Relative, pulse-to-pulse measurement (for > $10^{10}$ photons/pulse) |
| | 1% or better | After mirrors to measure reflectivity (0.2–25 keV) |
| Range | $10^{6}$–$10^{14}$ photons/s | |

## Photon beam position

The monitoring of the photon beam position has the following commissioning requirements:

- FEL radiation will be monitored shot to shot (time resolution 180 ns or better) and online, in both the x and y direction. (Spontaneous radiation will be imaged on a single-shot basis.)
- Two positions are required to determine photon beam pointing. The separation of the two monitors and their distance to the undulator should be as large as possible, but they should be placed upstream of the *K-monochromator*.
- Precision (accuracy is not required): ±10 µm for beam position variations within ±1 mm; $\delta x$=10 µm for a distance of 100 m between two monitors for 0.1 µrad angular resolution; and 1/10 of beam size sigma.
- XBPMs will have a relative accuracy of 0.2% of the beam diameter. Quadrant diodes and PIN diode arrays assist during commissioning.

During commissioning, two partially transparent solid-state BPMs with micrometre accuracy will also be suitable. They distort the wavefront of the beam, but, in return, offer good and pulse-resolved spatial resolution.

## Transverse beam profile, shape, and position

Complementing the pure beam position data from the XBPMs, a 2D beam viewer employing a scintillator or fluorescence screen will provide a beam profile and assist in beam-based alignment of components.

The 2D beam viewer will have the following accuracy:

- ± 5 µm (in 0.2–80 keV range) to align beamline optics using the X-ray beam
- ± 50 µm over a ± 5 mm range to align other components during commissioning

## Total energy in the radiation pulse and photon beam image

The total pulse energy has to be measured for detection and tuning of the SASE process over the range from spontaneous to FEL radiation, as shown in Table 10.

***Table 10:*** *Requirements for intrusive measurements of the total pulse energy*

| **Requirement** | **Value** |
|---|---|
| Relative accuracy | Better than 1% |
| Spatial resolution of MCP image | 30 µm |
| Photon energy range | 280 eV – 24.5 keV |
| Pulse energy range | 1 nJ – 10 mJ |

A combination of an MCP with a phosphor screen can provide a direct 2D image of the X-ray beam. The same is achieved by fluorescence in a Ce:YAG or doped diamond screen. Neither method will be able to resolve all pulses in a full pulse train, but serve as a single pulse mode tool for operators during commissioning and maintenance.

The MCP-based photon detectors will provide the following features:

- Measurement of the pulse energy
- Measurement of the photon beam image
- Operation at the pulse repetition rate of the European XFEL (10 Hz bunch train repetition rate, 4.5 MHz intra-bunch train repetition rate), thus resolving each individual radiation pulse

Three MCP stations will cover the following X-ray photon energy ranges:

- MCP1 at SASE1: 3–24 keV
- MCP2 at SASE2: 3–24 keV
- MCP3 at SASE3: 280 eV – 3 keV

The extended operating wavelength range is dictated by:

- Measurement of pulse energy in higher harmonics
- Operation of the European XFEL at reduced energy (10.5 GeV)

The design and calculations take into account an optional extension of the upper energy limit when using metal-coated mirrors (e.g. Palladium):

- Relative accuracy of measurements better than one per cent.
- Dynamic range of photon pulse energies between 1 nJ and 20 mJ. This applies for spontaneous and FEL radiation.
- Visualization with MCP imager, single bunch, or average over full train.
- Spatial resolution of MCP imager: 30 μm.

### Harmonic content

Intensities in the first, third, and higher harmonics will be simultaneously recorded to determine the harmonic content. An intrusive K-monochromator for undulator tuning, mainly used during commissioning, determines the spectral content in different harmonics. The spectral range should cover 10 to 15 harmonics.

### Spectrum

Measuring the spectral distribution is required for several purposes, as shown in Table 11. For comparison, the bandwidth of the *K-monochromator* Silicon crystal is 0.015%.

*Table 11: Spectral accuracy requirements*

| **0.28–3 keV** | **3–25 keV** | **purpose** |
|---|---|---|
| 0.01% | 0.01% | Energy calibration with electron beam |
| 0.1% | 0.01% | Undulator checks, BL transmission, monochromator setup |
| 0.001% within 0.1% | 0.0001% within 0.01% | Temporal structure |

# Operating requirements

Most commissioning requirements extend to the operation phase, but operation also brings some additional requirements. While some photon beam properties are less crucial for the startup of the SASE process, they are of rather high priority to users during operation. Explicitly, this concerns the polarization, temporal properties, and the wavefront.

## Polarization

The orientation and degree of linear polarization (or if provided by the undulators, the degree of circular polarization) will be monitored. Photoelectron spectroscopy is a promising technology for this task. User demand calls for a measurement accuracy of 1% for polarization degree.

## Temporal properties

Pump-probe experiments require synchronization at the sub-10 fs level. The accuracy of the beam arrival time should be < 1 %, and the pulse duration needs to be measured at a level of accuracy better than the length of the delivered pulses.

## Wavefront

Wavefront measurements will help to adjust transport and focusing optics. They will be used to determine FEL-induced changes in beamline optics and the FEL wavefront itself for use in experiments. The wavefront determination accuracy is required at a level of $\lambda/15$.

# References


[Alaimo2009]

M. D. Alaimo, M.A.C. Potenza, M. Manfredda, G. Geloni, M. Sztucki, T. Narayanan, M. Giglio: “Probing the Transverse Coherence of an Undulator X-ray Beam Using Brownian Particles”, Physical Review Letters **103**, 194805 (2009)

[Altarelli2006]

M. Altarelli et. al. (ed.): “The European X-ray Free Electron Laser Technical Design Report”, DESY 2006-091 (2006)

[Bergonzo2006]

P. Bergonzo, D. Tromson, C. Mer: “CVD diamond-based semi-transparent beamposition monitors for synchrotron beamlines: preliminary studies and device developments at CEA/Saclay”, J. Synchrotron Rad. 13, 151–158 (2006)

[Bionta2011]

M. Bionta et. al.: “Spectral encoding of X-ray/optical relative delay”, Optics Express Vol. 19, No. 22, 21855 (24 October 2011)

[Bittner2007]

Bittner et. al.: “MCP-based photon detector with extended wavelength range for FLASH”, Proceedings of FEL07, Novosibirsk, Russia (2007)

[Buck2012]

J.Buck, et. al.: “Conceptual Design Report: Photoemission Spectrometer”, in preparation

[Bytchkov2004]

A. Bytchkov et al.: “Development of MCP-based photon diagnostics at the TESLA Test Facility at DESY”, Nucl. Instrum. and Methods A **528**, 254 (2004)

[David 2011]

C. David, S. Gorelick, S. Rutishauser, J. Krzywinski, J. Vila-Comamala, V.A. Guzenko, O. Bunk, E. Färm, M. Ritala, M. Cammarata, D.M. Fritz, R. Barrett, L. Samoylova, J. Grünert, H. Sinn: “Nanofocusing of hard X-ray free electron laser pulses using diamond based Fresnel zone plates”, Scientific Reports **1**, Article 57 (2011)

[Ding2011]

Y. Ding, P. Emma, J. Frisch, Z. Huang, H. Loos, P. Krejcik, M-H. Wang, C. Behrens: “Ultra-short electron bunch and X-ray temporal diagnostics with an X-band transverse deflector”, Proceedings FEL11, Shanghai (2011)

[Emma2010]

P. Emma, et. al. “First lasing and operation of an angstrom-wavelength free-electron laser”, Nature Photonics, vol. **4**, 641 (2010)

[Feng2009]

Yiping Feng: Presentation on “LUSI Diagnostics & Common Optics” at the three-way SLAC, DESY, and SPring-8 collaboration meeting, February 2009

[Fuchs2008]

M. Fuchs, K. Holldack, M. Bullough, S. Walsh, C. Wilburn, A. Erko, F. Schäfers, U. Mueller: “Transmissive X-ray beam position monitors with submicron position- and submillisecond time resolution”, Rev. Sci. Instrum. **79**, 063103 (2008)

[Fuchs2008]

G. Geloni, E. Saldin, L. Samoylova, E. Schneidmiller, H. Sinn, Th. Tschentscher, M. Yurkov: “Coherence properties of the European XFEL”, New J. Phys., 12 (2010)

[Grünert2009]

J.Grünert: “Photon Diagnostics Requirements and Challenges at the European XFEL”, Proceedings FEL09, Liverpool (2009)

[Grünert2009-2]

J.Grünert, K.Tiedtke, A.Sorokin: “Considerations concerning the position of the XGMDs and XBPMs along the beamlines of the European XFEL”, internal report, 2 September 2009

[Hott 2011]

T. Hott: “Mandatory Documents for CDRs”, EDMS Document Number D00000002104281,C,1,2 (May 2011)

[Ischebek2004]

R. Ischebeck, M. Tonutti, J. Feldhaus, C. Gerth, E. Saldin, E. Schneidmiller, K. Tiedtke, R. Treusch, P. Schmüser, M. Yurkov: “Measurement of the transverse coherence of a VUV Free Electron Laser”, Proceedings of EPAC 2004, Lucerne, Switzerland

[Ishikawa2010]

T. Ishikawa, M. Yabashi et. al.: “XFEL/SPring-8 Beamline Technical Design Report” (2010)

[Ishikawa2010]

P. Moritz, E. Berdermann, K. Blasche, H. Stelzer, B. Voss: “Broadband electronics for CVD-diamond detectors”, Diamond and Related Materials **10**, 1765-1769 (2001)

[Kohlstrunk2011]

N. Kohlstrunk et al.: Beamlines Component List, EDMS-Nr.: D00000002629421 Rev: A Ver: 1, 19 December 2011

[Li2012]

B. Li et. al.: “Conceptual design report for a parasitic temporal diagnostics at the European XFEL”, in preparation

[Micron2009]

Micron Semiconductor Ltd., West Sussex, UK: *Catalogue 2009*, www.micronsemiconductor.co.uk,

[Ozkan2012]

C. Ozkan et. al.: “Conceptual Design Report: Imaging Stations for Invasive Photon Diagnostics at the European XFEL”, in preparation

[Paganin1998]

D.Paganin and K.A.Nugent: “Noninterferometric phase imaging with partially coherent light”, Phys.Rev.Lett. **80**, 2586-2589 (1998)

[Pomorski2009]
M. Pomorski, M. Ciobanu, C. Mer, M. Rebisz-Pomorska, D. Tromson, P. Bergonzo: “Position-sensitive radiation detectors made of single crystal CVD diamond”, Phys. Status Solidi A 206, No. 9, 2109–2114 (2009)

[Rehanek2011]
J. Rehanek, F. Schaefers, A. Erko, M. Scheer, W.Freund, J.Gruenert, C. Ozkan, S. Molodtsov: “Simulations of diagnostic spectrometers for the European XFEL using the ray-trace tool RAY”, Proc. SPIE Vol. 8141, 814109 (2011)

[Schäfer2002]
B. Schäfer, K. Mann: “Determination of beam parameters and coherence properties of laser radiation by use of an extended Hartmann-Shack wave-front sensor”, Applied Optics Vol.**41** No.15, 2809 (2002)

[Schulze-Briese2001]
C. Schulze-Briese, B. Ketterer, C. Pradervand, Ch. Brönnimann, C. David, R. Horisberger, A. Puig-Molina, H. Graafsma: “A CVD-diamond based beam profile monitor for undulator radiation”, Nucl. Instrum. and Methods A **467–468**, 230–234 (2001)

[Sorokin2011]
A.A. Sorokin, U. Jastrow, S. Bonfigt, K. Tiedtke: “XGMD final design”, European XFEL / DESY Internal Report (2011)

[Syresin2011]
E. Syresin et. al.: “XFEL MCP detectors”, European XFEL Internal Report, JINR, Dubna, Russia (2011)

[Tiedtke2008]
K. Tiedtke et al.: “Gas detectors for X-ray lasers”, J. Appl. Phys. **103**, 094511 (2008)

[Tono2011]
K. Tono, T. Kudo, M. Yabashi, T. Tachibana, Y. Feng, D. Fritz, J. Hastings, T. Ishikawa: “Single-shot beam-position monitor for X-ray free electron laser”, Rev.Sci.Inst. **82**, 023108 (2011)

[Tschentscher 2011]
T. Tschentscher: “Layout of the X-Ray Systems at the European XFEL”, XFEL.EU TR-2011-001 (2011) www.xfel.eu/documents/technical_documents/

[Volkov 2011]
Pavel Volkov: “Shot-to-Shot Backscatter Monitor for Intensity-Position Measurement at the European XFEL”, Internal XFEL.EU Report, 8 September 2011

[Yabashi 2006]
M. Yabashi, J. Hastings, M. Zolotorev, H. Mimura, H. Yumoto, S. Matsuyama, K. Yamauchi, and T. Ishikawa: “Single-Shot Spectrometry for X-Ray Free-Electron Lasers”, Phys. Rev. Lett. **97**, 084802 (2006)

# Annexes

The following annexes to this document contain organizational information about WP74 and will be provided upon authorized requests:

- WP74 budget
- WP74 staffing plan

# Acknowledgements

We would like to thank the following people, groups, and institutions:

- X-Ray Photon Diagnostics group (WP74 at European XFEL) for input to this document, discussions, reviews and more: Cigdem Ozkan, Jens Buck, Wolfgang Freund, and Bin Li
- Colleagues at European XFEL who contributed with discussions, advice, and input data, most prominently Harald Sinn of WP73
- Kurt Ament for assistance in formatting and proofreading this manuscript
- Institutes and groups that will contribute devices, especially the group of Kai Tiedtke at HASYLAB (DESY) and the group of Evgeny Syresin at JINR in Dubna
- Groups who provide simulation support for diagnostics devices, namely Gianluca Geloni with WP72 at XFEL.EU, as well as Alexei Erko, Franz Schäfers, and Jens Rehanek at the Helmholtz Center Berlin
- Many scientific collaborators who are mentioned in this report

In addition, we would like to note the following:

- WP74 work is carried out under the responsibility of Serguei Molodtsov, Scientific Director and member of the Management Board of European XFEL.
- We acknowledge the financial support by the European XFEL GmbH and its international shareholders.